AIP Applied Physics Letters

Logic-memory device of a mechanical resonator

Atsushi Yao and Takashi Hikihara

Citation: Applied Physics Letters **105**, 123104 (2014); doi: 10.1063/1.4896272
View online: http://dx.doi.org/10.1063/1.4896272
View Table of Contents: http://scitation.aip.org/content/aip/journal/apl/105/12?ver=pdfcov
Published by the AIP Publishing

APPLIED PHYSICS LETTERS 105, 123104 (2014)

Logic-memory device of a mechanical resonator

Atsushi Yao[1,a)] and Takashi Hikihara[1,b)]
Department of Electrical Engineering, Kyoto University, Katsura, Nishikyo, Kyoto 615-8510 Japan

(Received 28 July 2014; accepted 10 September 2014; published online 22 September 2014)

We report multifunctional operation based on the nonlinear dynamics in a single microelectromechanical system (MEMS) resonator. This letter focuses on a logic-memory device that uses a closed loop control and a nonlinear MEMS resonator in which multiple states coexist. To obtain both logic and memory operations in a MEMS resonator, we examine the nonlinear dynamics with and without control input. Based on both experiments and numerical simulations, we develop a device that combines an OR gate and memory functions in a single MEMS resonator.
 [http://dx.doi.org/10.1063/1.4896272]

Microelectromechanical systems or nanoelectromechanical systems (MEMS or NEMS) resonators have been developed for use as filters, frequency references, and sensor elements.[1] Recently, significant research has focused on mechanical computation based on MEMS or NEMS resonators.[2–17] Some studies have shown that a single mechanical resonator can be used as a mechanical 1-bit memory[2,3,5,7,8,11–13,15] or as mechanical logic gates.[6,9,10] Recently, multifunctional operation has been demonstrated in the form of a shift-register and a controlled NOT gate made from a single mechanical resonator.[17] The next phase is to use a closed loop control to generate multifunction devices, which consist of memory and multiple-input gates, in a single device. The closed loop allows output and excitation signals to be fixed at a single frequency. The goal of the work presented in this letter is to develop multifunction operation from a nonlinear MEMS resonator in which multiple states coexist with closed loop control.

Nonlinear dynamical responses are commonly observed in a microelectromechanical or nanoelectromechanical resonator. The nonlinear dynamics of the resonator is well known to be described by the Duffing equation.[2,8,12,18–20] Such a nonlinear resonator has hysteretic characteristics, which lead to two stable states and one unstable state, depending on the frequency[1,21] or excitation force.[6,15]

This letter focuses on fabricating a multifunction device that offers logic and memory (called a "logic-memory device"). To do this, we examine the nonlinear dynamics in a MEMS resonator with and without control input. In the following, we discuss the experiments and numerical simulations that allowed us to develop a device that combines multiple-input gate and memory functions in a single nonlinear MEMS resonator.

The proposed comb-drive MEMS resonator is shown in Fig. 1. The resonator consists of a perforated mass with a width, length, and thickness of 175, 575, and 25 μm, respectively.[19,22,23] When the comb-drive resonator is electrically excited, the mass vibrates in the lateral direction. The vibration of the mass is detected by using a differential measurement[24] in vacuum (around 10 Pa) at room temperature. The output voltage of the differential measurement is $V_{\mathrm{out}} = 7.2\,\mathrm{Vsm}^{-1} \times f_{\mathrm{e}} v_{\mathrm{ace}} A_{\mathrm{e}} \sin(4\pi f_{\mathrm{e}} t + \phi_{\mathrm{e}})$, where A_{e} denotes the displacement amplitude, ϕ_{e} is the phase, f_{e} is the excitation frequency, and v_{ace} ($= 0.6$ V) is the ac excitation amplitude. The vibration displacement is measured without additional sensors; therefore, the MEMS resonator is equipped with a comb drive that normally serves as a forcing actuator, but which simultaneously serves as a displacement sensor.[11,16]

Figure 2(a) shows the amplitude frequency response (without control input u_{e}). The MEMS resonator produces a hysteretic response: the curves differ for increasing and decreasing frequency sweeps. The nonlinear dynamics of the MEMS resonator is qualitatively modeled as follows:

$$\frac{\mathrm{d}^2x}{\mathrm{d}t^2} + \frac{2\pi f_0}{Q}\frac{\mathrm{d}x}{\mathrm{d}t} + (2\pi f_0)^2 x + \alpha_3 x^3 = 4.0\,\mathrm{m}(\mathrm{Vs}^2)^{-1} \times (V_{\mathrm{dcn}} + u_{\mathrm{n}})\sin 2\pi f_{\mathrm{n}} t, \qquad (1)$$

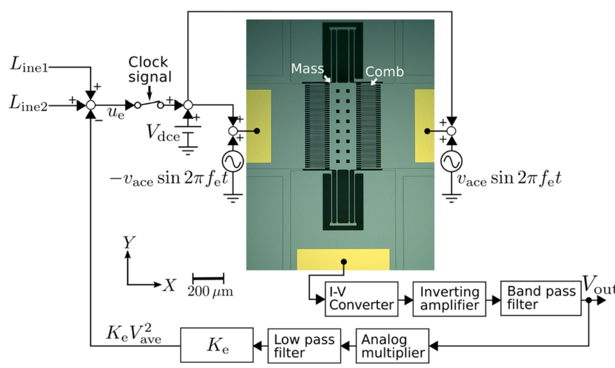

FIG. 1. Schematic of MEMS resonator, measurement system, and control system that relates to logic inputs. The nonlinear MEMS resonator, fabricated using silicon-on-insulator technology, is actuated by an ac excitation voltage v_{ace} with a dc bias voltage V_{dce}. When the MEMS resonator is excited, the mass vibrates in the X-direction. In the measurement system, the output voltage V_{out} depends on the amplitude and phase of the displacement in the nonlinear MEMS resonator. The control system is implemented with a feedback input and logic inputs. The feedback input is given as the slowly changing dc voltage V_{ave}^2, to which the output voltage V_{out} is converted by an analog multiplier and a low-pass filter (see Ref. 11 for more details). The time constant of the low-pass filter is set to about 0.47 s. The logic inputs, represented by two dc voltages (L_{ine1} and L_{ine2}), are added to the dc bias voltage V_{dce}. As a result, the excitation force under control becomes proportional to $V_{\mathrm{dce}} + u_{\mathrm{e}} = V_{\mathrm{dce}} + L_{\mathrm{ine1}} + L_{\mathrm{ine2}} - K_{\mathrm{e}} V_{\mathrm{ave}}^2$. Here L_{ine1} and L_{ine2} denote the input signals, which serve as the logic inputs, u_{e} is the control input, and K_{e} ($= 11\ \mathrm{V}^{-1}$) is the feedback gain in the experiments.

[a)]Electronic mail: yao@dove.kuee.kyoto-u.ac.jp
[b)]Electronic mail: hikihara.takashi.2n@kyoto-u.ac.jp

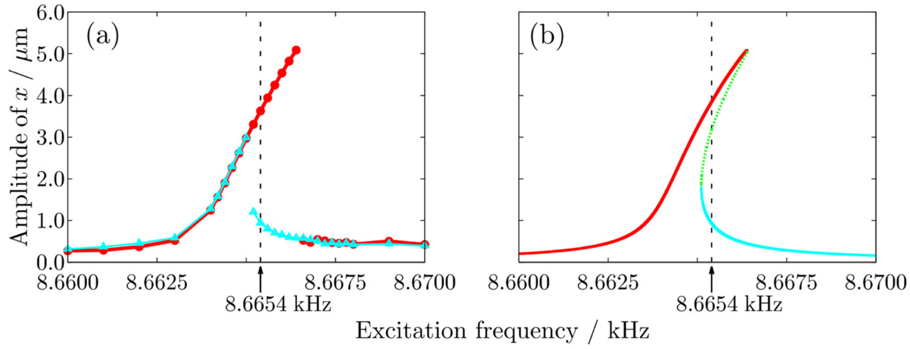

FIG. 2. (a) Experimentally obtained frequency response curves at $V_{dce} = 150$ mV and $u_e = 0.0$ mV. The dark (red) and thin (aqua) lines correspond to the responses to increasing and decreasing frequency sweeps, respectively. In the hysteresis region, two coexisting stable states appear that strongly depend on the sweep direction. (b) Corresponding numerical response curves generated from Eq. (1) for $V_{dcn} = 150$ mV and $u_n = 0.0$ mV. The solid (red and aqua) lines show two stable solutions and the dashed (green) line shows an unstable solution.

where x denotes the displacement, f_n is the excitation frequency, $f_0\,(= 8.6644$ kHz) is the resonance frequency, $Q\,(= 25\,000)$ is the quality factor, $\alpha_3\,(= 7.06 \times 10^{16}\ (\mathrm{sm})^{-2})$ is the nonlinear mechanical spring constant, V_{dcn} is the dc bias voltage, and u_n is the control input. The parameters are obtained based on our reported parameter estimation method.[25] Fig. 2(b) shows the amplitude as a function of excitation frequency for the resonator as determined by numerical simulations at $V_{dcn} = 150$ mV and $u_n = 0.0$ mV. At any given frequency in the hysteretic region, the MEMS resonator exhibits two coexisting stable states. In the following experiments and simulations, the excitation frequency is fixed at 8.6654 kHz.

Figure 3(a) shows the experimentally determined hysteretic behavior as a function of dc bias voltage V_{dce} at $u_e = 0.0$ mV. The corresponding numerical results are shown in Fig. 3(b) with respect to numerical dc bias voltage V_{dcn}. The hysteresis region exists at 95 mV $< V_{dce} <$ 275 mV in Fig. 3(a) and 105 mV $< V_{dcn} <$ 245 mV in Fig. 3(b). The difference of hysteresis regions is caused by noise in Fig. 2(a). The nonlinear MEMS resonator has stable regions (solid line) that are completely separated by an unstable region (dashed line). These stable regions, which correspond to large and small amplitude vibrations, define the two states of the single-output logic or memory device in a single MEMS resonator. In the numerical simulations and experiments, a displacement amplitude greater than 3.0 μm is regarded as a logical "1"; a value less than 3.0 μm is regarded as a logical "0" for logic and memory output. Hereinafter, the numerical and experimental dc bias voltages (V_{dcn} and V_{dce}) are fixed at 150 mV.

We now discuss the nonlinear dynamics with control input as a logic operation. Fig. 1 shows the control system to perform the logic operation. The switching between two coexisting stable states was done by a displacement feedback control in the nonlinear MEMS resonator.[11] Based on the results, the feedback control is performed. The logic inputs are applied to the MEMS resonator in the form of two dc voltages (L_{ine1} and L_{ine2}). In the experiments, the control input u_e is described as follows:

$$u_e = L_{ine1} + L_{ine2} - K_e V_{ave}^2, \tag{2}$$

where K_e denotes the feedback gain and V_{ave}^2 is a slowly changing dc voltage that depends on the displacement.[11]

The corresponding numerical control input u_n is described as follows:[12]

$$u_n = L_{inn1} + L_{inn2} - K_n A_{nave}^2, \tag{3}$$

$$A_{nave}^2 = \frac{A_{n1}^2 + A_{n2}^2 + \cdots + A_{nm}^2 + \cdots + A_{nM}^2}{M}, \tag{4}$$

where L_{inn1} and L_{inn2} denote the input signals that are the logic inputs, K_n is the feedback gain, m is a natural number,

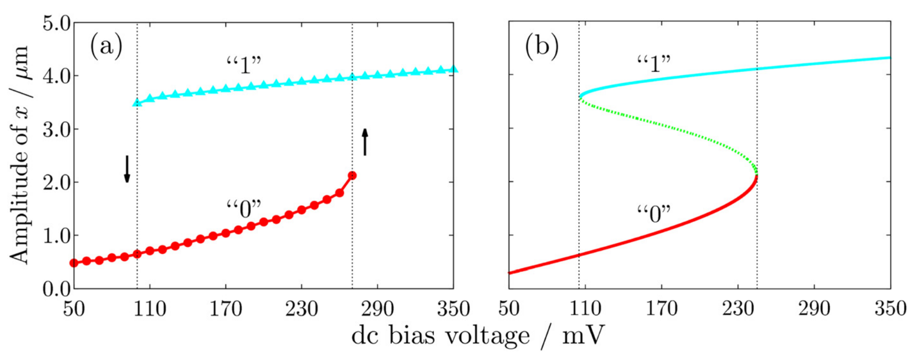

FIG. 3. (a) Measured hysteretic characteristics with respect to dc bias voltage V_{dce} at 8.6654 kHz and $u_e = 0.0$ mV. The excitation amplitude in the absence of the control input is proportional to the dc bias voltage V_{dce}. The experimentally obtained response shows the hysteretic behavior when the excitation amplitude is swept from left to right (thick red line) and right to left (thin aqua line). For logic and memory output, the thin (dark) line is regarded as a logical "1" (logical "0"). (b) Corresponding numerical hysteretic characteristics as a function of dc bias voltage V_{dcn} at $f_n = 8.6654$ kHz. The solid (red and aqua) lines show stable regions and the dashed (green) line shows an unstable region. These stable regions can be used as two states, corresponding to logical "0" and "1," for logic and memory functions, as in panel (a).

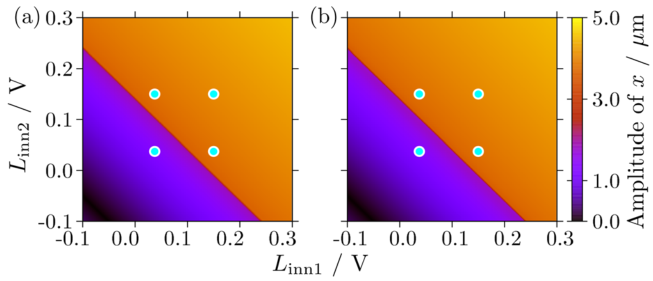

FIG. 4. Amplitude modulation systematically varied in input signals $L_{\rm inn1}$ and $L_{\rm inn2}$ at $f_{\rm n} = 8.6654$ kHz and $V_{\rm dcn} = 150$ mV (numerical results). The light (dark) region corresponds to more than (less than) 3.0 μm in displacement amplitude, corresponding to a logical "1" (logical "0") output. For an OR gate, input signals are set to 150.0 mV and 37.5 mV, as shown by the four circles with light (aqua) color: (a) Initial state is set to the large amplitude solution (logical "1" for memory output) (b) Initial state is the small amplitude solution (logical "0" for memory output).

M is the average number, and $A_{{\rm n}m}$ is the displacement amplitude of the previous m period within $1 \le m \le M$ for the numerical simulations. In this case, $A^2_{\rm nave}$ is the average of $A^2_{{\rm n}m}$. $K_{\rm n}$ is set to 1.42×10^{10} Vm^{-2} and M is set to 22 000.

Figure 4 shows the numerically obtained steady states when the control input is applied to the MEMS resonator. The control input can induce a modulation of the resonator's amplitude and thus change the logical value of the output. In Fig. 4(a) (Fig. 4(b)), the initial state of memory output is a logical "1" (logical "0"). In Figs. 4(a) and 4(b), there exist regions in which the displacement amplitude is the same because the control system depends on the feedback input. Assume that the control system receives just the input signals $L_{\rm inn1}$ and $L_{\rm inn2}$. When the input signals $L_{\rm inn1} = L_{\rm inn2} = 0.0$ mV are sent to the MEMS resonator, the large stable state cannot switch to the small state. Therefore, a single MEMS resonator can be used as a logic gate because of the adjustment of the logic inputs and the feedback input.

To execute a memory operation in a MEMS resonator, we must consider the nonlinear dynamics without the control input. When the control input is not applied, every initial state corresponds to the convergence to either the small amplitude (black) or large amplitude (white) solutions, as shown in Fig. 5. In the nonlinear MEMS resonator, the small and large amplitude solutions have each basin of attraction[26] around each solution. The convergence conditions depend on the two basins of attraction.[8,12] The light region (displacement amplitude greater than 3.0 μm) in Fig. 4 corresponds to white region in Fig. 5 and vice versa. When the control input is not applied, the MEMS resonator maintains its original logic output. Thus, the nonlinear MEMS resonator works as the memory device by storing the logic information.

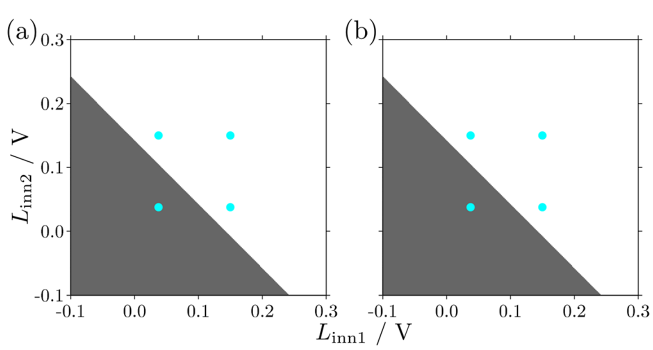

FIG. 5. Calculated convergence conditions (final state) when the control input shown in Fig. 4 is off. The white (black) region corresponds to convergence to a logical "1" (logical "0") for memory output. Light (aqua) circles show the logic input in our simulations, as in Fig. 4: (a) Numerical results corresponding to Fig. 4(a). (b) Numerical results corresponding to Fig. 4(b).

The results shown in Figs. 4 and 5 indicate that MEMS resonator works as a combined logic-memory device. The logic and memory operations can be programmed by adjusting the resonator's operating parameters (input signals). In the numerical simulations, when the input signal ($L_{\rm inn1}$ or $L_{\rm inn2}$) is set to 150.0 mV (37.5 mV), the logic input is regarded as logical 1 (logical 0). The logic inputs (0, 0) of input signals ($L_{\rm inn1}$, $L_{\rm inn2}$) have a value of 75.0 mV, (0, 1) and (1, 0) have a value of 187.5 mV, and finally (1, 1) have 300.0 mV, as shown by the light (aqua) circles in Figs. 4 and 5. The output of the device is a logical "0," when the logic inputs are (0, 0), which correspond to a value of 75.0 mV. However, when the logic inputs are set to (0, 1), (1, 0), or (1, 1), the output corresponds to a logical "1." Therefore, the single MEMS resonator combines the function of an OR gate and memory.

These logic and memory operations can be demonstrated experimentally in a single MEMS resonator. The operations are confirmed for the behavior of device at clock evolution. The calculated time evolutions of the device are shown in Fig. 6(a) and the corresponding experimental time evolutions are shown in Fig. 6(b). The calculated results are consistent with the experimental results. When electrical noise and surges appear in Fig. 6(b), no logic faults occur and the memory operations are not perturbed. The experimental modulation of the amplitude and the convergence conditions will be examined in more detail in a future presentation. When the excitation frequency changes, it is anticipated that desired operations of OR gate and memory cannot be achieved. Nevertheless, this work demonstrates both experimentally and numerically a combined device of OR gate and memory functions in a single MEMS resonator.

Here, we estimate an instantaneous power of the MEMS resonator. In Fig. 1, when the voltages of right electrode are excited by $v_1 = V_{\rm dce} + v_{\rm ace} \sin 2\pi f_{\rm e} t$ and the left by $v_2 = V_{\rm dce} - v_{\rm ace} \sin 2\pi f_{\rm e} t$, the right and left comb capacitances (C_1 and C_2) are given by $C_1 = 5.75 \times 10^{-9}\,{\rm Fm}^{-1} \times (l + A_{\rm e} \sin(2\pi f_{\rm e} t + \phi))$ and $C_2 = 5.75 \times 10^{-9}\,{\rm Fm}^{-1} \times (l - A_{\rm e} \sin(2\pi f_{\rm e} t + \phi))$, where $A_{\rm e}$ denotes the displacement amplitude and $l\,(= 100\ \mu{\rm m})$ is the initial overlap between the fingers.[11] The power of the MEMS resonator p is described by $p = v_1 \partial(C_1 v_1)/\partial t + v_2 \partial(C_2 v_2)/\partial t$. In this study, $l v^2_{\rm ace}$ is much greater than $A_{\rm e} V_{\rm dce} v_{\rm ace}$. Thus, the power is estimated as $1.13 \times 10^{-8} \sin 4\pi f_{\rm e} t$ W.

In conclusion, we numerically and experimentally demonstrated a multifunctional device consisting of a nonlinear MEMS resonator. We confirmed that when a control input is applied to a nonlinear MEMS resonator, two equal-amplitude regions exist because of the adjustment of the feedback input. Therefore, a single MEMS resonator can work as an OR gate. We also used numerical simulations to show that in the absence of the control input, the nonlinear MEMS resonator maintains its original logical state. Thus, this resonator also serves as a memory device. Therefore, we demonstrate a

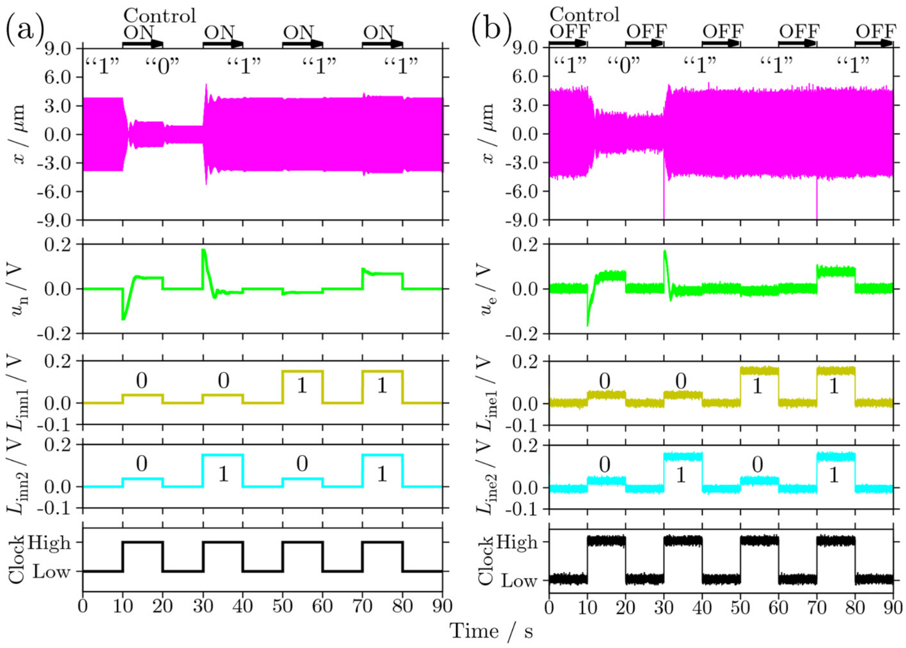

FIG. 6. Time evolution of the combined device (OR gate and memory). The initial memory output is a logical "1." When the clock signal is high (low), the control input is (is not) applied to the MEMS resonator. Note that the nonlinear MEMS resonator is used as a logic (memory) device at high (low) clock signal. The logic inputs start from (0, 0) and continue to (0, 1), (1, 0), and (1, 1). The logic output in a MEMS resonator changes to logical "0," "1," "1," and "1" at each high clock signal: (a) Numerical results. (b) Experimental results. In our experiments, the logic input 1 (0) of experimental input signal (L_{ine1} or L_{ine2}) has a voltage of 150.0 mV (37.5 mV).

combination of an OR gate and a memory device in a single MEMS resonator. Mahboob *et al*. have developed a device that combines a controlled NOT gate and memory functions in a single resonator at 2 K.[17] In this letter, we realize a logic-memory device of high reliability operating at room temperature with the logic inputs given as two dc voltages that do not depend on the phase. By considering the closed loop and bias inputs, these results open the way to further research in high and multi functionality in single and coupled resonators, which may take the form of multiple-input gates such as three- or four-input logic gates and memory.

We are grateful to Professor S. Naik (Weber State University, USA) for his support in the design of MEMS resonators and Mr. Y. Umezaki (Graduate Student, Kyoto University) for discussions about parameter settings. This work was partly supported by the Global COE of Kyoto University, Regional Innovation Cluster Program "Kyoto Environmental Nanotechnology Cluster," and the JSPS KAKENHI (Grant-in-Aid for Exploratory Research) No. 21656074. One of the authors (A.Y.) was supported by the Grant-in-Aid for JSPS Fellows No. 26462.

[1]V. Kaajakari, *Practical MEMS* (Small Gear Publishing, 2009).
[2]R. L. Badzey, G. Zolfagharkhani, A. Gaidarzhy, and P. Mohanty, Appl. Phys. Lett. **85**, 3587 (2004).
[3]R. L. Badzey and P. Mohanty, Nature (London) **437**, 995 (2005).
[4]S. C. Masmanidis, R. B. Karabalin, I. De Vlaminck, G. Borghs, M. R. Freeman, and M. L. Roukes, Science **317**, 780 (2007).
[5]I. Mahboob and H. Yamaguchi, Nat. Nanotechnol. **3**, 275 (2008).
[6]D. N. Guerra, A. R. Bulsara, W. L. Ditto, S. Sinha, K. Murali, and P. Mohanty, Nano Lett. **10**, 1168 (2010).
[7]H. Noh, S.-B. Shim, M. Jung, Z. G. Khim, and J. Kim, Appl. Phys. Lett. **97**, 033116 (2010).
[8]Q. P. Unterreithmeier, T. Faust, and J. P. Kotthaus, Phys. Rev. B **81**, 241405 (2010).
[9]I. Mahboob, E. Flurin, K. Nishiguchi, A. Fujiwara, and H. Yamaguchi, Nat. Commun. **2**, 198 (2011).
[10]D. Hatanaka, I. Mahboob, H. Okamoto, K. Onomitsu, and H. Yamaguchi, Appl. Phys. Lett. **101**, 063102 (2012).
[11]A. Yao and T. Hikihara, IEICE Electron. Express **9**, 1230 (2012).
[12]A. Yao and T. Hikihara, Proc. NOLTA **2012**, 352.
[13]N. A. Khovanova and J. Windelen, Appl. Phys. Lett. **101**, 024104 (2012).
[14]J.-S. Wenzler, T. Dunn, T. Toffoli, and P. Mohanty, Nano Lett. **14**, 89 (2014).
[15]A. Uranga, J. Verd, E. Marigó, J. Giner, J. L. Muñóz-Gamarra, and N. Barniol, Sens. Actuators, A **197**, 88 (2013).
[16]A. Yao and T. Hikihara, Phys. Lett. A **377**, 2551 (2013).
[17]I. Mahboob, M. Mounaix, K. Nishiguchi, A. Fujiwara, and H. Yamaguchi, Sci. Rep. **4**, 1 (2014).
[18]R. M. C. Mestrom, R. H. B. Fey, J. T. M. van Beek, K. L. Phan, and H. Nijmeijer, Sens. Actuators, A **142**, 306 (2008).
[19]S. Naik, T. Hikihara, H. Vu, A. Palacios, V. In, and P. Longhini, J. Sound Vib. **331**, 1127 (2012).
[20]D. Antonio, D. H. Zanette, and D. López, Nat. Commun. **3**, 806 (2012).
[21]J. A. Pelesko and D. H. Bernstein, *Modeling MEMS and NEMS* (Chapman & Hall/CRC, 2003) Chap. V.
[22]S. Naik and T. Hikihara, IEICE Electron. Express **8**, 291 (2011).
[23]S. Naik, "Investigation of synchronization in a ring of coupled MEMS resonators," Ph.D. dissertation (Kyoto University, 2011).
[24]V. Kempe, *Inertial MEMS: Principles and Practice* (Cambridge University Press, 2011) Chap. VI.
[25]Y. Umezaki, A. Yao, and T. Hikihara, Proc. IEICE Gen. Conf. **A-2-7**, 32 (2014) (in Japanese).
[26]J. Guckenheimer and P. Holmes, *Nonlinear Oscillations, Dynamical Systems, and Bifurcations of Vector Fields* (Springer, 1983).